A quantitative study of the practical sensitivity limit of a terahertz absorption spectrometer[†]

Jon E. Bjarnason[a‡], Charles Dietlein[a,b] and Erich N. Grossman[a]

[a]Optoelectronics Division, National Institute of Standards and Technology
Mailcode 815.04 : 325 Broadway, Boulder, CO 80305-3328.
[b]Department of Electrical and Computer Engineering, 425 UCB,
University of Colorado at Boulder, Boulder, CO, 80309

ABSTRACT

In gas spectroscopy, chemicals can be identified by the set of frequencies at which their absorption lines occur. The concentration can be quantitatively estimated from the intensity of any of the absorption lines. The sensitivity of the spectrometer, i.e., the minimum detectable concentration, is ideally limited by the ratio of the source power to detector noise-equivalent power. In practice, the sensitivity is usually orders of magnitude worse due to systematic effects. In this work we built a simple gas terahertz transmission spectrometer to analyze how the source output power stability, the detector sensitivity, and atmospheric pressure affect its sensitivity. As a test gas we used methyl chloride in a mixture with air and modifid the widths of the absorption lines by changing partial pressure of air. This demonstration of a simple absorption spectrometer gives us insight into the approach to making a highly sensitive terahertz spectrometer.

Keywords: Linewidth, methyl chloride, pressure broadening, spectroscopy,.

1. INTRODUCTION

The use of terahertz spectroscopy for trace gas detection has recently been addressed through both the more recent time-domain[1] and the more classical frequency-domain[2] approaches. The general advantages of the terahertz region, particularly in terms of specificity, are discussed in both references. Specificity requires low gas pressure to reduce line broadening (when lines broaden too much they become indistinguishable), so these terahertz techniques are best suited for point-sensing rather than remote sensing. The simplest technique is frequency-domain, continuous-wave (CW) direct absorption spectroscopy. This technique and several representative applications of it are surveyed by Gorshunov et al.[3] and the application to detection of chemical agents discussed by Bousquet et al.[4] In all implementations of a direct absorption spectrometer, the minimum detectable concentration is fundamentally limited only by source power, detector sensitivity, and effective path length. In practice, however, various systematic effects often limit the minimum detectable concentration to values that are orders of magnitude higher (worse) than this fundamental limit. Unfortunately, the exact nature of these systematic effects is often unclear, so the relationship between the spectrometer's actual sensitivity and the performance of its individual components is often unknown. In this work we explore a basic CW terahertz spectrometer, with special emphasis on the absolute intensity of the absorption lines of a molecular species rather than their linewidth. We then reduce the concentration of the test species to see what the sensitivity limits are.

2. THEORY

The terahertz transmission, T, through a sample is governed by the Lambert-Beer law:

$$T(\upsilon) = e^{-d\alpha(\upsilon)} \quad , \tag{1}$$

[†] Contribution of the U.S. government; not subject to copyright.
[‡] E-mail: jeb@askur.org , phone: +1 805 729 3705

where $\alpha(v)$ is the frequency-dependent attenuation coefficient and d is the path length. If collision events in the gas are Poisson distributed and the angular momenta before and after collisions are not correlated, then the absorption line shape around the frequency v_0 is described by the Lorentzian function,

$$\alpha(v)=I_0\Gamma \{ (v - v_0)^2 + (\Gamma /2)^2\} /2\pi, \tag{2}$$

where Γ is the full-width-at-half-maximum (FWHM) linewidth. Eq. (2) is normalized to the so-called total intensity

$$I_0 = \int_0^\infty \alpha(v)dv$$

. The total intensity is independent of the width, and therefore the linewidth and peak absorption must be inversely proportional:

$$\alpha_{PEAK} = \frac{2I_0}{\pi\Gamma} . \tag{3}$$

The spectrometer in this work uses a tunable CW terahertz source and a pyroelectric broadband sensor. In this way, the frequency can be tuned while transmitted power is monitored by the detector. We expect the detected voltage, U_1 at each frequency, v, to be proportional to the source power, P_1 and the gas transmission (Eq. 1):

$$U_1(v)=R P_1(v)exp\{-d\alpha(v)\} , \tag{4a}$$

with a proportionality constant, R, that is the voltage responsivity of the detector. In order to extract the attenuation spectrum, $\alpha(v)$, we need to measure the power from the source again, P_2, in the absence of the attenuator ($\alpha=0$) as a reference spectrum:

$$U_2(v)=R P_2(v) . \tag{4b}$$

The sensitivity of the detector, R, is assumed to be constant over time. The uncertainties in the spectra ΔU_1 and ΔU_2, come from (1) the explicit voltage uncertainty ΔV of the detector, and (2) the implicit voltage uncertainty due to the source power, i.e., $R\Delta P_{source}$:

$$\Delta U_1=R \Delta P_{source} exp\{-d\alpha\} + \Delta V, \tag{5a}$$

and

$$\Delta U_2=R \Delta P_{source} + \Delta V. \tag{5b}$$

Therefore the uncertainty in the absorption coefficient $\alpha=-\ln(U_1 / U_2)/d$ is the Pythagorean sum of the uncertainty contributors:

$$\Delta\alpha=1/d \{ [1+exp(2\alpha d)](\Delta V/U_2)^2 + 2 (R\Delta P/U_2)^2\}^{1/2} . \tag{6}$$

The voltage uncertainty of the detector in the noise equivalent bandwidth NEBW, is determined from the voltage power spectral density S_V of the detector, $(\Delta V)^2= S_V \cdot NEBW$ (where S_V is measured in V^2/Hz). The power uncertainty is similarly determined from the power power spectral density of the source, $(\Delta P)^2= S_P \cdot NEBW$ (where S_P is measured in W^2/Hz). The power spectral densities can be obeserved by measuring the voltage power spectral density of the detector, S, with the source on ($S=S_V+R^2 S_P$) and off ($S=S_V$).

Eq. 6 shows that that higher source power and longer path length are beneficial, and that the source power uncertainty (repeatability, drift, noise, etc.) is just as important as the noise equivalent power of the detector, S_V/R, when the attenuation is weak. Special techniques are often employed to get an effectively larger d. These include reflecting the beam between parallel mirrors and using resonant cavities. One of the challenges in spectroscopy is measuring a reference spectrum without affecting parameters other than the presence of the sample, in other words, making sure that $P_1=P_2$.

3. EXPERIMENTAL SET-UP.

The spectroscopy measurements were performed with a backward-wave oscillator (BWO) source and a pyroelectric infrared sensor (pyro). The BWO output power was 0.15 +/- 0.02 mW at 877 GHz. The pyroelectric sensor was integrated with a transimpedance amplifier, the output of which was measured with a lock-in amplifier. The lock-in amplifier was phase-locked with a mechanical chopper at the output waveguide of the BWO. An off-axis parabola was
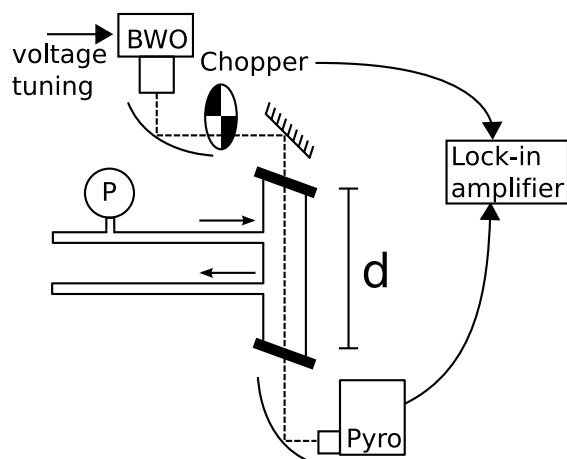
Figure 1. A terahertz gas spectrometer. A voltage tunable backward wave oscillator terahertz source (BWO), is collimated with a parabolic mirror and aimed through a gas cell of length d, with angled Brewster windows. The gas cell is connected to a pressure gauge, P, a gas supply, and a vacuum pump. The transmitted power is measured by a pyroelectric detector by basic lock-in amplifier techniques.

used to collimate the terahertz beam. The beam was then aligned with a stainless steel tube having 40 mm diameter, connected to a vacuum pump and a plumbing network that supplied gases and monitored pressure. The pressure was monitored with a convection gauge calibrated for air down to 10^{-2} Pa.

Each end of the gas sample tube had an off-normal polyethylene window (n=1.5 @ 450 GHz[5]) to avoid spectral undulations due to standing waves between the windows. In addition, the window tilt angle was chosen to correspond to the Brewster angle (56.3º) to minimize reflective losses from the source to the detector.

4. METHYL CHLORIDE.

Methyl chloride (CH_3Cl) is a good sample gas to use to evaluate spectrometer operation because its dipole moment, 1.87 Debye[6], is typical for polar covalent bonds (water having 1.85 Debye). The HITRAN[7,8] molecular database lists a total of 12775 pure rotational lines below 2200 GHz for methyl chloride. Since the chemical contains a chlorine isotope, the spectrum can actually be visualized as a superposition of two spectra of two isotopomers that occur in the abundance of 0.748 (^{35}Cl) and 0.239 (^{37}Cl). The isotope ^{A}Cl is identified by its mass number, A. The amplitude of the absorption of each isotopomer scales with its abundance, and the frequency of $CH_3^{37}Cl$ is redshifted with respect to $CH_3^{35}Cl$ because of its larger moment of inertia. In the HITRAN database, CH_3Cl is categorized as a symmetric rotor, and all the transitions in the terahertz range involve the vibrational ground state. The lowest vibrational transition occurs

Table 1. HITRAN parameters for two absorption bands in $CH_3^{35}Cl$ and $CH_3^{37}Cl$. The integrated intensity is the sum of the intensities of all the lines in the respective J band. The peak center is the frequency of the largest peak within each J band.

Spectral parameter	Value		Unit
Average molar mass	50.49		g/mol
Cl mass number, A	35	37	
Abundance	0.748	0.239	
J (ang. mom. q.n.)	36→35	37→36	
Peak Intensity	$4.5 \cdot 10^{-20}$	$1.3 \cdot 10^{-20}$	GHz/molec.cm^{-2}
Peak center	954.2	965.5	GHz
Integrated intens.	$7.8 \cdot 10^{-19}$	$2.3 \cdot 10^{-19}$	GHz/molec.cm^{-2}
Weighted center freq.	954.094	965.356	GHz
Density @300K 100 Pa	$2.4 \cdot 10^{22}$	-	molec./m^3
Γ_{self} @ 102.4 kPa	8.916	8.556	GHz (HWHM)
Γ_{air} @ 102.4 k Pa	2.538	2.478	GHz (HWHM)

above our range of interest, or at 20.22 THz. This makes the terahertz spectrum of CH_3Cl simpler than the spectrum of water. Each bar in Figure 2 represents a rotational transition of one iosotopomer where the angular momentum quantum number, J, decreases by 1. When we take a closer look at each J-line (Fig. 2 inset), we see that they split up into a manifold or band of very closely spaced lines that are indexed by another angular momentum quantum number K. Fig. 2 shows the J=36→35 transition band of the common isotopomer. The highest intensity line in the J=36→35 transition is tabulated as $4.5 \cdot 10^{-20}$ GHz/(molec.cm^{-2}) but the accumulated intensity over all K's in the band is $7.8 \cdot 10^{-19}$ GHz/(molec.cm^{-2}) and the intensity weighted center of the band is at 954.2 GHz. We use the ideal gas law $PV=nk_BT$ to derive the molecular density, $n/V=p/(k_BT)$, from the pressure. Table 1 lists a number of HITRAN parameters.
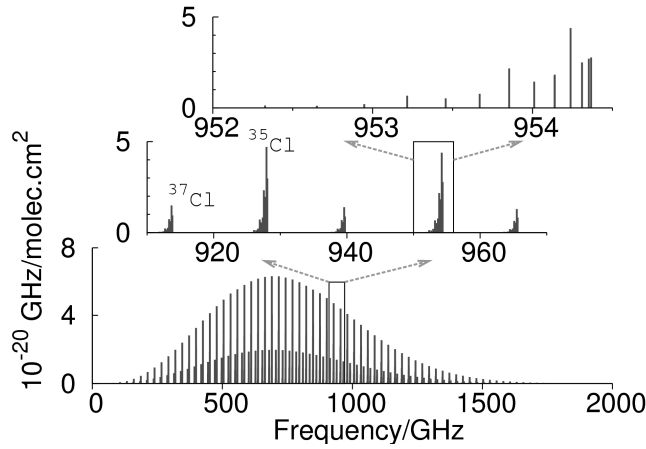

Figure 2. The HITRAN lines for CH_3Cl. All these transition are in the vibrational ground state. The third (top) expanded spectrum contains the 36→35 band of the $CH_3{}^{35}Cl$ isotopomer.
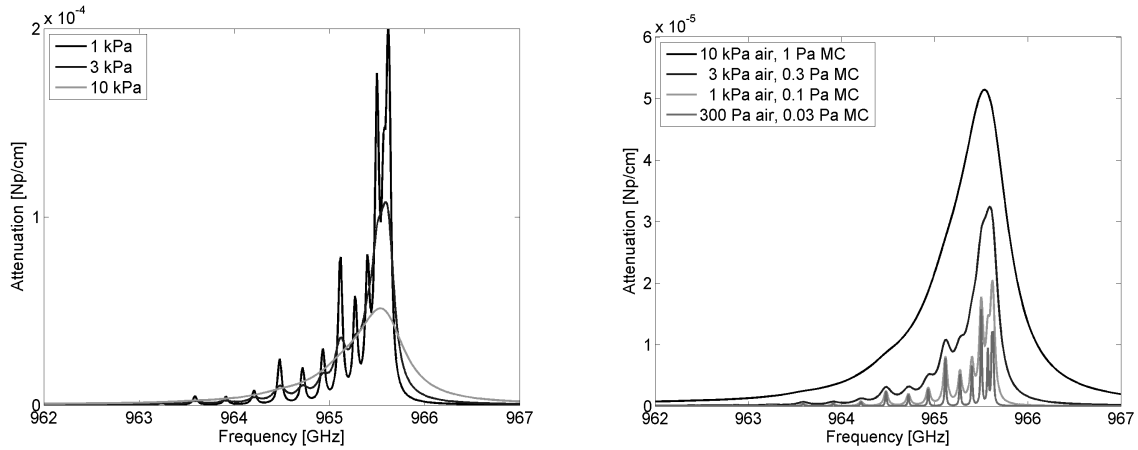

Figure 3. Left: Simulation of the absorption spectrum for which the CH_3Cl pressure is kept constant at 1 Pa while the air pressure is reduced. While the air broadening decreases the peak intensity goes up. The integrated intensity remains the same. Right: This simulates a situation where 1 Pa CH_3Cl (MC) is in a mixture with 10 kPa air and the total pressure is reduced.

The pressure broadening of CH_3Cl is modeled by an air-broadening factor, Γ_{air}, and a self-broadening factor, Γ_{self}, weighted by their partial pressures p_{air} and p_{self}:

$$\Gamma(p) = \Gamma_{air} p_{air} + \Gamma_{self} p_{self} \,. \tag{7}$$

The self broadening factor is more than 3 times larger than the air-broadening factor. Fig. 3 shows the 954 GHz band when all the absorption lines in the band have been broadened and summed over for particular pressures.

5. RESULTS AND DISCUSSION

A. System characterization.

Fig 2 shows typical operating parameters of the transmission spectrometer. The pyroelectric detector unit was calibrated in the infrared with a hot infrared source, but its responsivity at 950 GHz is actually unknown. According to the application notes, it has a broad spectral range 0.001 to 1000 μm in wavelength, but the flatness of the response is specified only up to 100 μm. The coupling from the BWO through the gas sample cell and into the pyroelectric detector was less than 10 %. We attribute this mostly to the small active area of the pyro sensor (1 mm^2). The BWO cathode is electrically heated with a DC source that switches polarity every 13.67 seconds. Since the BWO output power depends slightly on the heater polarity, the frequency tuning and data acquisition were synchronized with the heater period. In other words, the frequency was stepped at each rising edge on the heater current polarity. In that way the heater has the same effect on both the sample spectrum and the reference spectrum.

The frequency of the BWO depends on the cathode voltage. The voltage-frequency tuning curve was mapped out by measuring frequency, ν, at discrete cathode voltages, V_C, with an interferometer which had 0.3 GHz resolution. The slope of the tuning curve and the curvature ($d^2\nu/dV_C^2$) are shown in Table 2. Although the BWO tuning curve shifts over time we assume that the slope is the same. The absolute frequency of the BWO could be verified as often as needed by measuring a spectrum of known CH_3Cl transitions.

The spectrometer accuracy was estimated observing the statistics of 10 second, 80 sample segments (oversampled) at the output of the lock-in amplifier, which had a single pole filter with 300 ms time constant. The noise equivalent bandwidth of a 10 s sample average is $(4\cdot10s)^{-1}=0.025$ Hz. First, the BWO was blocked, measuring only the pyro detector voltage noise. This resulted in a standard deviation of 0.4 μV. When the BWO was unblocked the pyro detector read 1.4 mV and the standard deviation was 1 μV (6 μV/Hz$^{1/2}$). The increase in noise with the BWO source turned on is attributed to short-term (timescale unknown, but less than 10 s) power amplitude noise in the BWO source. The

Table 2. Experimental parameters.

| Parameter	Value	Units
Modulation freq.	25	Hz
Pyro Sensitivity @ 25 Hz	1300	V/W @ 25 Hz
Pyro area	1	mm^2
Pyro noise power spectral density at 24 Hz	3	μV/Hz$^{1/2}$
Lock-in time constant	300	ms single pole RC
Sample rate	8	Hz
Sampling interval	10	s
BWO tuning period	13.67	s
BWO cathode voltage	3700	V
BWO tuning slope @3.7 kV	104.2	MHz/V
BWO tuning curvat.	0.02	MHz/V^2
Path length in gas, d	36.8	cm
Approximate beam diam.	3	cm
Gas cell diameter	4.0	cm
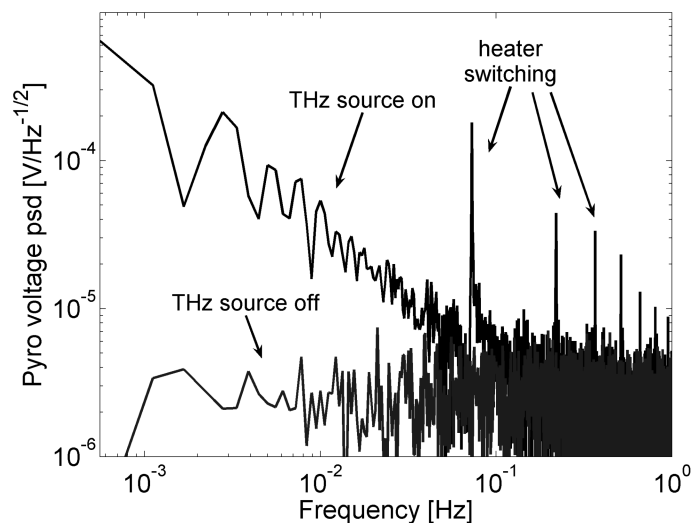
Figure 4. The power spectral density measured at the output of the lock-in amplifier with the BWO turn on and off. Below 0.1 Hz the noise contribution from the BWO dominates over the pyro voltage noise. The periodic spikes are the BWO 13.67 second cathode heater switching and all the harmonics.

BWO power spectrum (power vs. cathode voltage) was repeated 10 times over a period of 3 hours, while evacuating and refilling the sample cell with 9.4 kPa of air each time. This gave an estimate of the repeatability of consecutive gas transmission spectra measurements. The three-hour repeatability had a standard deviation of 20 µV, and the best repeatability came from spectra within 10 minutes, with a standard deviation of 4 µV. Another indicator of the long-term stability of the system can be seen by taking a Fourier transform of a long term-time sequence of the BWO power measured by the pyro detector, see Fig. 4.

From Eq. 6, and comparing the detector with the repeatability noise, we see that for small attenuation, the uncertainty is dominated by the BWO power fluctuations on a timescale comparable to the period needed to refill the sample cell.

B. Spectroscopy measurement.

In the first measurement, the total pressure was chosen to be high enough (~10 kPa) that the spectrum acquisition was less sensitive to frequency error. In this limit, the air broadening (460 MHz) dominates the self broadening (10.5 MHz), and all the K lines in each J band smear out due to broadening. The spectrometer frequency range was set to measure the $J=37 \rightarrow 36$ band of the less common isotopomer. By using the less common isotopomer we reached the sensitivity limit of the spectrometer without having to measure low pressures accurately.

The measurement was performed by evacuating the gas cell down to 0.1 Pa. Then CH_3Cl was injected into the gas cell until the desired partial pressure was reached. After that, air was let in until the desired total pressure (~10 kPa) was reached. When a spectrum had been acquired, a reference spectrum was measured as soon as possible afterwards by evacuating the cell again down to 1 Pa and filling with air up to the total pressure of the CH_3Cl measurement. In this way the total pressure in the cell was the same for the sample spectrum and the reference spectrum. A reference spectrum at vacuum would have provided a methyl-chloride-free reference spectrum, but the sample cell coupling would have been distorted because of the 10 kPa pressure deflecting the polyethylene windows. For the 130 Pa total pressure measurements, described in the following subsection, a vacuum reference spectrum was sufficient because that pressure does not deflect the window.

The left side of Fig. 5 shows 9 spectra at decreasing CH_3Cl partial pressures from 63 to 0 Pa. In each spectrum, the absorption intensity drops without any visible change in the width. The accumulated intensity of each of these spectra was calculated and plotted against the partial pressure corrected for CH_3Cl on the right side plot of Fig. 5. The linear relationship between intensity and partial pressure, which has a slope of $2.1 \cdot 10^{-3}$ NpGHz/Pa, confirms that the pressure

gauge is linear in this range and the gas mixing is performed correctly. This curve was used to adjust the air calibration curve of the pressure gauge for CH_3Cl, because calibration curves for CH_3Cl were not provided from the manufacturer. The standard deviation in the measured attenuation, αd, at each frequency point is $\alpha d=0.005$ Np. Therefore the uncertainty in the intensity integrated (by summation) over the frequency range is 0.012 Np GHz. Thus the minimum detectable pressure using this absorption line and this system (essentially 25 dB SNR) at 965 GHz is 0.005 NpGHz/($2.1 \cdot 10^{-3}$ Np/Pa)=2.5 Pa.

Since the most significant data points lie where the absorption peaks are, the least-squares error estimator weights the signal in the absorption peak higher. The least-squares error problem is stated as:

$$\alpha_i = pM_i + \varepsilon_i, \tag{9}$$

where the unknown parameter p is the partial pressure, α_i's are the set of measured absorption coefficient at frequencies f_i, M_i are the HITRAN model absorption coefficients at 1 Pa partial pressure (calculated using Eq. 2) and ε_i are the observation errors in each measurement of α_i. We assume ε_i are independent and are normally distributed. The least-squares estimator of the partial pressure is

$$p = \frac{\sum_i \alpha_i M_i}{\sum_i M_i^2} \times 1 \text{ Pa}, \tag{10}$$

and its standard deviation with respect to the standard deviation of the data points, σ_α, is

$$\sigma_p = \sqrt{\frac{\frac{1}{20}\sum_i \sigma_{\alpha_i}^2}{\sum_i M_i^2}} \times 1 \text{ Pa}. \tag{11}$$

This gives a detectable pressure of 1 Pa for the 9.4 kPa case, which is equivalent to a detectable integrated intensity of 0.004 Np·GHz and 2.5 times better than the previous estimate with a uniform integral. Therefore the sensitivity is approximately 100 parts per million compared to the total pressure.

In a second measurement we chose the more abundant isotopomer, $CH_3{}^{35}Cl$ under a total pressure low enough to resolve the spread in the J=36→35 band. The measured spectra are shown in Fig. 6 (left) together with the corresponding HITRAN model. The air pressure, which is 135 Pa, anchors the FWHM of the lines to 7 MHz. From Eq. 3 we see that, because of the line narrowing, the peak absorption per unit pressure should increase by a factor of 21 compared with the

Table 3. Experimental results measuring 10 kPa air broadened J=37→36 band of $CH_3{}^{37}Cl$.

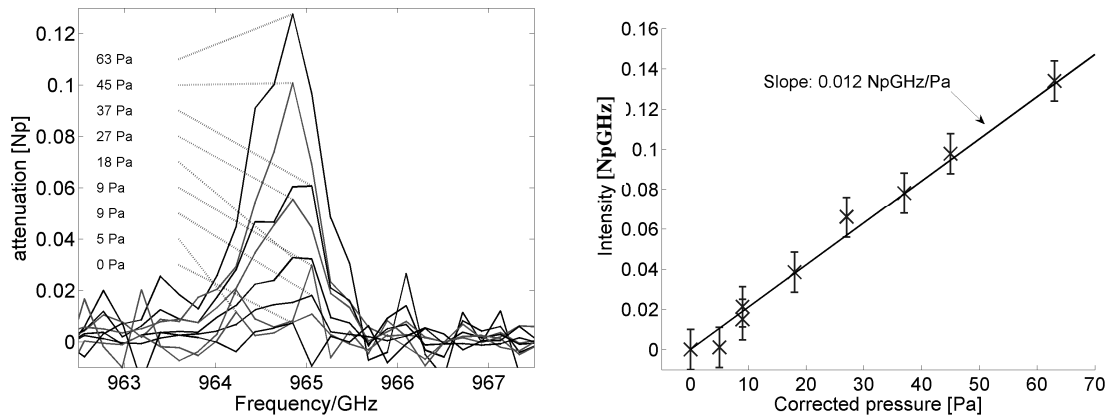| Parameter	Value
Air pressure	9.4 kPa
Frequency range	962.5-967.7 GHz
HITRAN integr. Intens.	0.002 NpGHz/Pa
Frequency step size	208 MHz
Air broadening (FWHM)	455 MHz
CH3Cl broad. @ 63 Pa	10.5 MHz
Total acquisition time	500 s
Detectable pressure	2.5 Pa
Detectable p least squares	1 Pa

Figure 5. Left: Normalized attenuation spectra of $CH_3{}^{37}Cl$ (J=37→36) at 9.4 kPa total pressure. Right: Integrated intensity of the spectra on the left figure vs. pressure of CH_3Cl. We used this to calibrate our pressure gauge based on HITRAN intensities.

previous high pressure measurement (up by 69 because of pressure broadening and down by a factor of 3.1 due to the isotope ratio). The low-pressure spectral measurement was made difficult by random unpredictable jumps in the frequency of the BWO. Therefore we decided to scan over three peaks so that we had a pattern as a frequency indicator. The step size (5.2 MHz) was barely enough to resolve the peaks. The absorption is obvious at a partial pressure of 0.9 Pa but 0.09 Pa was the lowest pressure for which the lines were clearly visible. The integrated line intensities are listed in Table 4.

Fig. 6 (right) shows a spectrum of $CH_3{}^{35}Cl$ at 0.04 Pa partial pressure. The $5 \cdot 10^{-4}$ Np error bars shown originate from the uncertainties in the power measurement at each point. However, we can see from the spectrum that systematic errors due to the repeatability of the BWO frequency tuning cause fluctuations that are larger than the power measurement uncertainty. From analyzing the statistics of multiple spectra we estimate that the uncertainty in the measurement of each α_i is roughly 0.003 Np, and thus from Eq. 11 the standard deviation in the partial pressure estimator is 0.02 Pa, corresponding to an integrated line strength of $5 \cdot 10^{-5}$ Np·GHz. The spectrum in Fig. 6 (right) is therefore only slightly above the detection limit.

Table 4. Experimental results measuring 135 Pa air-broadened J=36→35 lines of $CH_3{}^{35}Cl$.

| Parameter	Value
Air pressure	135 Pa
Frequency range	104 MHz
Step size	5.2 MHz
Total acquisition time	500 s
Air broadening (135 Pa, FWHM)	6.7 MHz
Self broadening (1 Pa, FWHM)	17 kHz
HITRAN integrated 954.29-954.39GHz	$2.6 \cdot 10^{-3}$ NpGHz/Pa
HITRAN total J=36→35 band	0.0187 NpGHz/Pa
0.9 Pa measurement integ. intensity	$1.8 \cdot 10^{-3}$ NpGHz
0.09 Pa measurement integ intens.	$2.3 \cdot 10^{-4}$ NpGHz
Sensitivity limit	$7 \cdot 10^{-5}$ NpGHz
Smallest measurable CH_3Cl press.	0.03 Pa
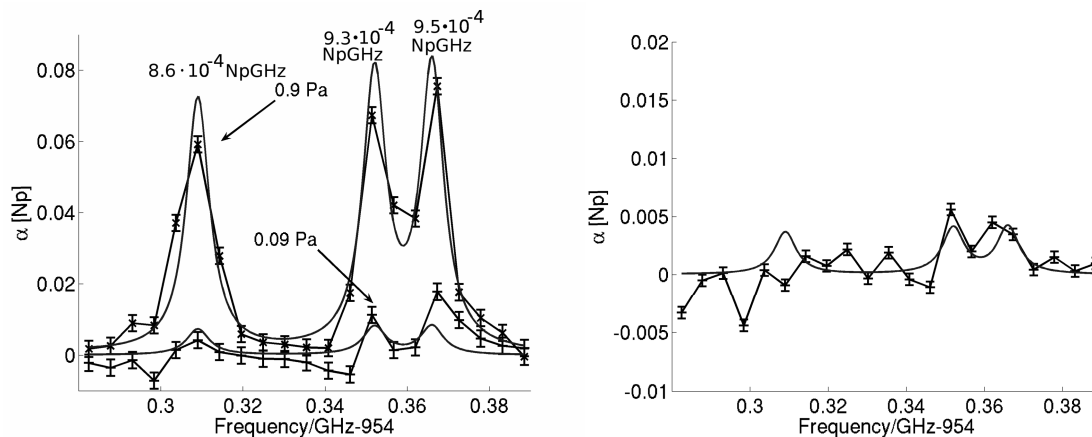
Figure 6. Left: Two normalized spectra of $CH_3{}^{35}Cl$ (J=36→35) at 0.9 Pa and 0.09 Pa. The HITRAN model calculated at the respective pressure is also plotted for comparison. The line intensity of each line is shown above each line. The sum of the intensities is 0.0027 NpGHz. The total pressure in these measurements was 135 Pa. Right: The absorption spectrum of 0.04 Pa partial pressure $CH_3{}^{35}Cl$ along with the HITRAN model at 0.06 Pa partial pressure.

We see that the improvement in sensitivity due to the pressure narrowing is a factor of 30. In comparing this measurement at 135 Pa with the previous measurement at 9.5 Pa, three factors are different: (1) the linewidth decreased by a factor of 69, (2) the fractional isotope concentration increased by a factor of 3.1, and (3) we are observing only three J,M lines, which constitute only 14.5 % of the J band. As a result, the parts per million of total pressure is close in the two measurements, or 150 vs. 100 parts per million.

6. CONCLUSION

We built a simple open-loop-frequency-tunable CW terahertz gas spectrometer and made an effort to reduce systematic errors. The largest contribution to the uncertainty in the line width was the repeatability error in the reference spectrum. Lowering the air pressure made each line narrower and the center absorption larger. The best sensitivity using a 36.8 mm total effective path length was 150 parts per million of the total pressure. It is theoretically possible to get a higher sensitivity by narrowing the lines even more, but that is more demanding in terms of frequency accuracy and stability. The fundamental barrier to line narrowing the Doppler linewidth (1.7 MHz FWHM for this molecule around 950 GHz), is not far from being reached, and at that point, amplitude fluctuations of the BWO will become limiting once again.

REFERENCES

1. S. A. Harmon, and Cheville, R.A., "Part-per-million gas detection from long-baseline THz spectroscopy," *Appl. Phys. Lett.*, vol. 85, pp. 2128, 2004.
2. I. R. Medvedev, Behnke, M., and DeLucia, F.C., "Fast Analysis of Gases in the Submillimeter/Terahertz with "Absolute" Specificity," *Appl. Phys. Lett.*, vol. 86, pp. 154105, 2005.
3. B. Gorshunov, Volkov, A., Spektor, I., Prokhorov, A., Mukhin, A., Dresse and M. , Uchida, S., and Loidl, A., "Terahertz BWO-Spectroscopy " *Intl. J of Infrared and Millimeter Waves*, vol. 26, pp. 1217-1240, 2005.
4. R. R. Bousquet, Chu, P.M., DaBell, R.S., Grabow, J-U., and Suenram, R.D., "Trends in Microwave Spectroscopy for the Detection of Chemical Agents," *IEEE Sensors J.*, vol. 5, pp. 656-664, 2005.
5. J. W. Lamb, "Miscellaneous data on materials for millimetre and submillimetre optics," *International Journal of Infrared and Millimeter Waves*, vol. 17, no. 12, pp. 1997-2034, December 1996.
6. A. N. M. Barnes, D. J. Turner, and L. E. Sutton, "Total electric polarizations of several polar gases," *Trans. Faraday Soc.*, vol. 67, pp. 2902-2906+, 1971.
7. L. S. Rothman, D. Jacquemart, A. Barbe, Chris, M. Biork, L. R. Brown, M. R. Carleer, J. Chackerian, K. Chance, L. H. Coudert, V. Dana, V. M. Devi, J. M. Flaud, R. R. Gamache, A. Goldman, J. M. Hartmann, K. W. Jucks, A. G. Maki, J. Y. Mandin, S. T. Massie, J. Orphal, A. Perrin, C. P. Rinsland, M. A. H. Smith, J. Tennyson, R. N. Tolchenov, R. A. Toth, Vander, P. Varanasi, and G. Wagner, "The HITRAN 2004 molecular spectroscopic

database," *Journal of Quantitative Spectroscopy and Radiative Transfer*, vol. 96, no. 2, pp. 139-204, December 2005.

8. L. S. Rothman, "The HITRAN molecular spectroscopic database and hawks (hitran atmospheric workstation): 1996 edition," pp. 665-710, November.